

THE INSTITUTE OF PAPER CHEMISTRY, APPLETON, WISCONSIN

**IPC TECHNICAL PAPER SERIES
NUMBER 250**

BUILDING A MECHANISTIC MODEL OF KRAFT-ANTHRAQUINONE PULPING KINETICS

M. A. BURAZIN AND T. J. McDONOUGH

JULY, 1987

Building a Mechanistic Model of Kraft-Anthraquinone Pulping Kinetics

M. A. Burazin and T. J. McDonough

Portions of this work were used by MAB as partial fulfillment of the requirements for the Ph.D. degree at The Institute of Paper Chemistry.

This paper will be presented at the TAPPI Pulping Conference in Washington, DC on November 1-5, 1987

Copyright, 1987, by The Institute of Paper Chemistry

For Members Only

NOTICE & DISCLAIMER

The Institute of Paper Chemistry (IPC) has provided a high standard of professional service and has exerted its best efforts within the time and funds available for this project. The information and conclusions are advisory and are intended only for the internal use by any company who may receive this report. Each company must decide for itself the best approach to solving any problems it may have and how, or whether, this reported information should be considered in its approach.

IPC does not recommend particular products, procedures, materials, or services. These are included only in the interest of completeness within a laboratory context and budgetary constraint. Actual products, procedures, materials, and services used may differ and are peculiar to the operations of each company.

In no event shall IPC or its employees and agents have any obligation or liability for damages, including, but not limited to, consequential damages, arising out of or in connection with any company's use of, or inability to use, the reported information. IPC provides no warranty or guaranty of results.

BUILDING A MECHANISTIC MODEL OF KRAFT-ANTHRAQUINONE PULPING KINETICS

M. A. Burazin and T. J. McDonough
The Institute of Paper Chemistry
Appleton, Wisconsin 54912

ABSTRACT

A study of kraft-anthraquinone (AQ) pulping kinetics was conducted to develop a mechanistic model valid over the bulk and residual phases. A competitive sequential experimental design criterion was used to choose conditions for each pulping run. Iterations of experiment, data analysis, and choice of new experimental conditions were used to discriminate among candidate models and to obtain precise parameter estimates for the best models.

The best delignification model incorporated three parallel pathways for lignin solubilization, followed by a lignin condensation step and a residual delignification step in which the condensed lignin is dissolved. The best models for dissolution of cellulose, glucomannan and xylan comprised two parallel pathways for peeling, two for stopping, and one for chain cleavage.

INTRODUCTION

Recent years have seen considerable progress toward the goal of developing quantitative descriptions of the kinetics of kraft pulping that are both accurately predictive and mechanistically plausible. As yet, however, there exists no model that is fully capable of predicting the effects of the concentrations of sodium hydroxide, sodium sulfide, and anthraquinone, nor of temperature history and chip size, on the outcome of a kraft cook. This is particularly true in view of the importance of being able to predict rejects levels and other pulp properties determined by uniformity of delignification. To do so requires a model that accurately simulates the dynamics of mass and heat transfer as well as the kinetics of the important chemical reactions.

Previous efforts to formulate such comprehensive models have in many cases been limited by the availability of rate expressions for the chemical parts of the process. Accordingly, the study reported here was undertaken as an early part of a larger effort to construct a detailed dynamic simulation model applicable to both kraft and kraft-anthraquinone (AQ) pulping processes. Its intent was to experimentally develop expressions for the rates of removal of lignin, glucomannan, arabinoxylan and cellulose which could later be coupled with mass and heat transfer models to achieve the total process simulation. Further details may be found in a thesis describing the entire study (1).

Experimental conditions for the reaction kinetics study were determined using the joint design criterion (C) developed by Hill, Hunter, and Wichern (2) to drive a sequential experimental design. The process began with a small initial set of experiments, then iterated through a cycle of

experiment, data analysis, and choice of new experimental conditions. After each set of experiments, all the data were analyzed and used to determine the levels of the experimental variables (time, temperature and concentrations) that maximized the numerical value of the joint design criterion, C. At each iteration, C was optimized once each for lignin, cellulose, glucomannan, and xylan. The four C optimal points in experimental space were used for the next set of experiments. The cycle of experiment, analysis, and prediction continued until arbitrary stopping criteria were satisfied.

Joint design criterion C postulates the existence of a finite number of possible mechanistic models, one of which is assumed to be the correct representation of the system being studied. The parameters for each model are determined by fitting the models to the available data. Experimental conditions which maximize C compromise best between two component criteria, model discrimination (D) and parameter estimation (E).

The model discrimination criterion, D, is a normalized form of the "raw" discrimination criterion D_0 :

$$D = D_0/D_{0\max}, \quad (1)$$

where $D_{0\max}$ is the maximum value of D_0 over the operability region, OR, (experimental design space). D_0 is a weighted sum of the squares of the differences between all unique pairs of model predictions:

$$D_0 = 1/2 \sum_{i=1}^m \sum_{j=i+1}^m \pi_{in} \pi_{jn} a, \quad (2)$$

where

$$a = \frac{(v_i - v_j)^2 + (y_{in+1} - y_{jn+1})^2 (v + v_i + v + v_j)}{(v + v_i)(v + v_j)}$$

where m is the number of models, π_{1n} is the probability that model 1 is correct based on the first n runs, y_{1n+1} is the predicted value of y_{n+1} using model 1, v_1 is the variance of y_{1n} about y_u calculated from the first n runs, and v is the inherent variance of the process. The π 's are calculated from

$$\pi_{1n} = \frac{\pi_{1n-1} P_1}{\sum_{i=1}^m \pi_{in-1} P_i} \quad (3)$$

$$P_1 = \frac{e^a}{\sqrt{[2\pi(v + v_1)]}} \quad (4)$$

$$a = -\frac{(y_n - y_{1n})^2}{2(v + v_1)}$$

where p_1 is the probability density function for y_{n+1} using model 1.

D is optimal for experimental conditions where the responses of the candidate models disagree the most. Running D optimal experiments maximizes the likelihood that only one model will be able to fit both the data generated by the run and the prior data.

The parameter estimation criterion, E, increases the precision of the model parameters. E is the weighted sum of the individual E_j for each of m models

$$D = \sum_{j=1}^m \pi_{jn} E_j / E_{j\max} \quad (5)$$

where $E_{j\max}$ is the maximum value of E_j over OR. E_j is the determinant of the transpose product of an array composed of the partial derivatives of model 1 with respect to model 1's parameters

$$E_1 = |X'X| \quad (6)$$

$$X = \{x_{iu}\} \quad (7)$$

$$x_{iu} = \left. \frac{\partial f(p, v_u)}{\partial p_1} \right|_{p = P(1n)} \quad \begin{matrix} u=1,2,\dots,n \\ i=1,2,\dots,p \end{matrix} \quad (8)$$

where p_1 is the i th parameter, and $P(1n)$ are the parameters for model 1 based on the data from the first n runs. v_u are the independent variables for run u , and $f(p, v)$ is the predicted value of y given p and v .

E is optimal for conditions where the models are the most sensitive, i.e., where a small change in model parameters causes a big change in model prediction. Running E optimal experiments minimizes the confidence volume about the model parameters.

Simultaneous optimization of model discrimination and parameter estimation is accomplished by using the relative probability of the most likely model (π_b) to weight model discrimination against parameter estimation. The joint design criterion is

$$C = d D + e E \quad (9)$$

where d and e are weights ($d + e = 1$). The weights d and e are calculated from π_b

$$d = m (1 - \pi_b) / (m - 1) \quad (10)$$

$$e = 1 - d \quad (11)$$

where m is the number of models. If all models are equally likely to be correct ($\pi_b = 1/m$) then $d = 1$,

$e = 0$ (pure model discrimination). If the best model fits the data perfectly and the others not at all ($\pi_b = 1$) then $d = 0$, $e = 1$ (pure parameter estimation). As the experimental method proceeds, π_b increases, and C shifts from emphasizing D to emphasizing E.

RESULTS AND DISCUSSION

Sequential experimental design

The models were fitted using NONLINWOOD, a nonlinear regression program (3). A program named MDPE (Model Discrimination/Parameter Estimation) was written to optimize C.

The reaction kinetics study began with 12 runs - a five variable fractional factorial in eight runs plus four centerpoints. Three of the factorial runs were discarded, and later repeated, because of analytical difficulties experienced early in the experimental program. The variables were time, temperature, [NaOH], [NaSH], and [AQ]. The responses were lignin, cellulose, glucomannan, and xylan. Thereafter, NONLINWOOD was run once per model to fit the candidate models to the data and MDPE was run once per response to optimize C for each response. The four conditions obtained were used for the next set of runs. Ten iterations of the sequential design were performed, resulting in a total of 52 usable runs. Complete experimental data are given in Table 5 in the Appendix. The Appendix also includes plots of observed and predicted values (Fig. 3-6).

Many candidate models were considered for each response. For example, over 60 lignin models were considered at one time or another, although no more than 10 were entertained at any one time. As the reaction kinetic study progressed, inferior models were discarded and new models were postulated.

Each model represents a mechanistically plausible reaction scheme. For instance, carbohydrate models accounting for just the peeling reaction were considered as well as models accounting for simultaneous peeling, stopping, and cleavage. The reaction variables looked at include the order of species dissolution with respect to [species], [NaOH], [NaSH], and [AQ]. Almost all of the candidate models investigated used parallel reaction pathways due to the experimental observation that alkaline pulping proceeds in the absence of NaSH and/or AQ.

In each case, the best model was selected as described below. Plots of predicted vs. observed values may be found in the appendix.

Bulk and residual phase kinetics

The final product of the reaction kinetics study was a set of equations, valid during the bulk and residual phases, which describe the rate of change of lignin, cellulose, glucomannan and xylan contents. The equations below represent the best candidate model for each species and have been tested over a wide experimental space using experimental conditions specifically designed to weed out inferior candidates. The best lignin model consisted of the reaction network shown in Fig. 1.

The parameters and standard errors for the best lignin model are shown in Table 1.

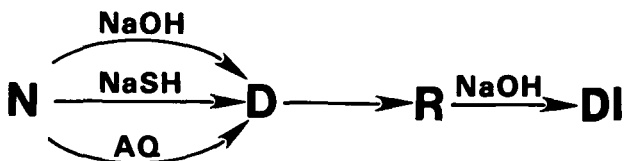


Fig. 1 Reaction network for best lignin model.

Table 1 Parameters for best lignin model

Name	Coefficient	Standard Error
k_{NDOH}	-4.15518	0.175
AE_{NDOH}	19608.7	1830
k_{NDSH}	-3.24838	0.158
AE_{NDSH}	10821.8	1130
k_{NDAQ}	-3.83789	0.236
AE_{NDAQ}	15897.1	2170
k_{DR}	-5.97332	0.352
k_{RD}	-6.00188	0.674
AE_{RD}	9991.03	2010

The network can be summarized as

$$\begin{aligned}
 \text{lignin} &= N + R \\
 \partial \text{lignin} / \partial t &= \partial N / \partial t + \partial R / \partial t \\
 \partial N / \partial t &= -k_{\text{bulk}} N \\
 \partial R / \partial t &= k_{\text{condense}} D - k_{\text{residual}} R \\
 \partial D / \partial t &= k_{\text{bulk}} N - k_{\text{condense}} D \quad (12)
 \end{aligned}$$

where N is native lignin, R is residual lignin, D is dissolved lignin, DI is inert dissolved lignin, and t is time in hr. Bulk delignification converts N to D, condensation converts D to R, and residual delignification converts R to DI. Bulk delignification was modeled as the sum of three parallel reaction pathways, dependent on NaOH, NaSH, and AQ:

$$\begin{aligned}
 k_{\text{bulk}} &= [\text{NaOH}] \sqrt{T} e^{(k_{NDOH} - AE_{NDOH} / T)} \\
 &+ \sqrt{[\text{NaOH}] [\text{NaSH}]} \sqrt{T} e^{(k_{NDSH} - AE_{NDSH} / T)} \\
 &+ \sqrt{[\text{NaOH}] [\text{AQ}]} \sqrt{T} e^{(k_{NDAQ} - AE_{NDAQ} / T)} \quad (13)
 \end{aligned}$$

where T is temperature in °K and brackets denote molar concentrations of the species they enclose, except for AQ, where they denote millimolar concentration.

Condensation was modeled as a single reaction pathway independent of [NaOH], [NaSH], and [AQ]. The condensation activation energy was fixed to a value expected for diffusion controlled reactions after attempts to fit the activation energy resulted in values approaching zero.

$$k_{\text{condense}} = \sqrt{T} e^{(k_{DR} - 2500 / T)} \quad (14)$$

Residual delignification was modeled as a single reaction pathway dependent on [NaOH].

$$k_{\text{residual}} = [\text{NaOH}] \sqrt{T} e^{(k_{RD} - AE_{RD} / T)} \quad (15)$$

The three carbohydrate fractions (cellulose, glucomannan, and xylan) were best modeled by the reaction network shown in Fig. 2. The parameters and standard errors for the best cellulose, glucomannan, and xylan models are shown in Tables 2, 3, and 4, respectively.

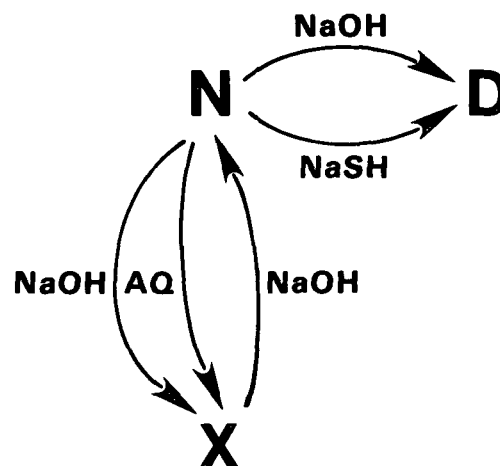


Fig. 2 Reaction network for best carbohydrate models.

Table 2 Parameters for best cellulose model

Name	Coefficient	Standard Error
k_{NDOH}	-5.04455	0.0784
AE_{NDOH}	6696.65	439
k_{NDSH}	-6.68305	0.233
AE_{NDSH}	8013.12	512
k_{NXOH}	-2.32248	0.0885
AE_{NXOH}	9611.41	378
k_{NXAQ}	-4.62038	0.0102
AE_{NXAQ}	16718.2	402
k_{XN}	-3.31930	0.0908

Table 3 Parameters for best glucomannan model

Name	Coefficient	Standard Error
k _{NDOH}	-0.857458	0.0809
A _{ENDO} H	6681.58	471
k _{NDSH}	-4.69499	0.343
A _{END} SH	12067.8	1890
k _{NXOH}	-1.51020	0.1135
A _{EN} XOH	3125.76	320
k _{NXAQ}	-2.35942	0.185
A _{EN} XAQ	10770.8	826
k _{XN}	-4.76589	0.112
A _E XN	12636.8	395

Table 4 Parameters for best xylan model

Name	Coefficient	Standard Error
k _{NDOH}	-2.303268	0.282
A _{ENDO} H	15595.18	1670
k _{NDSH}	-6.31659	0.190
A _{END} SH	2500	--
k _{NXOH}	-2.73932	0.505
A _{EN} XOH	8860.34	2460
k _{NXAQ}	-6.33924	2.46
A _{EN} XAQ	22304.0	10000
k _{XN}	-3.74624	0.318
A _E XN	12112.0	2220

The carbohydrate reaction network can be summarized as

$$C = N + X$$

$$\partial C / \partial t = \partial N / \partial t + \partial X / \partial t$$

$$\partial N / \partial t = k_{\text{cleave}} X - (k_{\text{peel}} + k_{\text{stop}}) N$$

$$\partial X / \partial t = k_{\text{stop}} N - k_{\text{cleave}} X \quad (16)$$

where C is cellulose, glucomannan, or xylan, N is the native fraction, D is the dissolved fraction, and X is the oxidized fraction. Peeling converts N to D, stopping converts N to X, and cleavage converts X back to N. The only distinction between N and X is that X does not peel. Peeling was modeled as two parallel reaction pathways dependent on NaOH and NaSH.

$$k_{\text{peel}} = [\text{NaOH}] \sqrt{T} e^{(k_{\text{NDOH}} - A_{\text{ENDO}}H / T)} + \sqrt{[\text{NaSH}]} \sqrt{T} e^{(k_{\text{NDSH}} - A_{\text{END}}SH / T)} \quad (17)$$

The activation energy for xylan peeling due to NaSH was fixed to a value expected for diffusion controlled reactions after attempts to fit the activation energy resulted in values approaching zero.

Stopping was modeled as two parallel reaction pathways dependent on NaOH and AQ.

$$k_{\text{stop}} = [\text{NaOH}] \sqrt{T} e^{(k_{\text{NXOH}} - A_{\text{EN}}XOH / T)} + [\text{NaOH}] \sqrt{[\text{AQ}]} \sqrt{T} e^{(k_{\text{NXAQ}} - A_{\text{EN}}XAQ / T)} \quad (18)$$

Cleavage was modeled as a single reaction pathway dependent on NaOH.

$$k_{\text{cleave}} = [\text{NaOH}] \sqrt{T} e^{(k_{\text{XN}} - A_{\text{E}}XN / T)} \quad (19)$$

Implications for kraft-AQ pulping

The fact that the models above were selected over many rejected models has several implications for an improved understanding of the kinetics of kraft-AQ pulping. Delignification is first order with respect to [lignin]. Cellulose, glucomannan, and xylan dissolution reactions are first order in [cellulose], [glucomannan], and [xylan], respectively. Models with inaccessible fraction parameters are inappropriate; the reaction kinetics study showed that these terms must equal zero for lignin, cellulose, glucomannan, and xylan.

Lignin networks consisting of bulk delignification, lignin condensation, and residual delignification reactions work much better than bulk delignification only schemes. Direct condensation of native lignin appears to be insignificant compared to condensation of dissolved lignin. Dissolved lignin appears to be able to condense with lignin or carbohydrate; models with a condensation rate dependence of {[lignin] x [dissolved lignin]} were inferior to models with a condensation rate dependence of [dissolved lignin]. Reaction schemes which included explicit conversion between native lignin and a reactive intermediate showed that the conversion rates were much faster than bulk delignification. Reaction schemes without the conversion reactions gave essentially the same results.

Carbohydrate networks consisting of simultaneous peeling, stopping, and cleavage reactions worked much better than peeling only networks. Carbohydrate peeling is accelerated by NaSH for all three carbohydrate fractions, the reaction rate being proportional to $\sqrt{[\text{NaSH}]}$. The carbohydrate stopping reaction is accelerated by AQ for all three fractions; the rate is proportional to $[\text{NaOH}] \sqrt{[\text{AQ}]}$.

CONCLUSIONS

Rate expressions for the removal of lignin, xylan, mannan, and cellulose during kraft-AQ or kraft

pulping have been identified by a sequential experimental technique.

The sequential experimental design strategy described above proved to be a very efficient method for conducting pulping kinetics studies. Five models were selected from over 200 candidate models in a 5-dimensional experimental space and their 43 parameters were estimated in only 52 runs. All parameters were significant at the 95% confidence level. A conventional 4-variable response surface study replicated in time would have required at least 250 runs.

The best kinetic models were chosen from many possible candidate models using experiments specifically designed to discriminate between the candidates. This is important, for it is all too easy to propose a particular reaction mechanism, develop an equation based on that mechanism, then generate plausible data that "prove" the mechanism.

EXPERIMENTAL

Details of the experimental method have been discussed previously (1).

Vacuum impregnated southern pine shavings were pulped at 40:1 l:w in a rotating multiunit digester. The internal temperature of each bomb was monitored continuously during the cook.

The pulp was washed, leached, extracted, then analyzed for lignin (4) and sugars (5).

ACKNOWLEDGMENTS

The authors wish to thank Mr. Art Webb, whose flexibility in scheduling the pulp analyses made

the sequential experimental design strategy possible.

We also wish to thank Drs. R. Halcomb, E. W. Malcolm and P. E. Parker for helpful discussions and sage advice.

Portions of this work were used by (MAB) as partial fulfillment of the requirements for the Ph.D. degree at The Institute of Paper Chemistry.

LITERATURE CITED

1. Burazin, M. A. "A Dynamic Model of Kraft-anthraquinone Pulping." Doctoral Dissertation. Appleton, WI, The Institute of Paper Chemistry, 1986.
2. Hill, W. J., Hunter, W. G., and Wichern, D. W. "A Joint Design Criterion for the Dual Problem of Model Discrimination and Parameter Estimation." Technometrics 10(1): 145-60(1968).
3. Daniel, C. and Wood, F. S. Fitting Equations to Data, 2nd edition. New York, NY, Wiley, 1981.
4. Effland, M. J. "Modified Procedure to Determine Acid-insoluble Lignin in Wood and Pulp." Tappi 60(10): 143-4(1977).
5. Borchardt, L. G. and Piper, C. V. "A Gas Chromatographic Method for Carbohydrates as Alditol-acetates." Tappi 53(2): 257-60(1970).
6. TAPPI Standard Test Method T236 os-76 Kappa Number of pulp.

APPENDIX

Table 5

Time, t, hr	Temp., T, °C	t to T, min	NaOH, mole/L	NaSH, mole/L	AQ, mmole/L	Lignin,	Cel, ^a ZODW	GM, ^a	Xylan,
--	--	--	--	--	--	30.0	39.2	16.1	8.95
--	--	--	--	--	--	30.0	38.8	16.6	8.84
--	--	--	--	--	--	30.2	38.4	16.8	8.41
--	--	--	--	--	--	30.1	38.0	17.2	8.51
1	27	--	1	0.2	1	28.4	40.3	16.4	8.04
1	27	--	1	0.2	1	28.2	40.7	16.8	8.54
1	27	--	1	0.2	1	28.2	37.6	16.6	7.06
1	27	--	1	0.2	1	28.5	39.2	17.6	8.55
1.367	130	16	0.501	0.099	0.502	21.5	38.4	7.16	7.30
4.228	130	16	2.007	0.099	2.007	14.2	35.4	8.80	5.12
4.228	130	16	0.511	0.402	0.507	16.2	38.7	7.18	7.00
1.367	130	16	2.018	0.402	1.989	19.9	37.1	9.80	6.27
4.299	170	18	2.018	0.402	0.507	0.177	21.0	1.63	0.184
2.390	150	17	1.002	0.198	1.007	6.19	33.8	6.01	2.98
2.390	150	17	1.002	0.198	1.005	5.53	35.8	6.82	3.07
2.390	150	17	1.002	0.198	0.999	5.61	38.9	7.20	3.50
2.390	150	17	1.002	0.198	1.006	5.93	39.6	7.29	3.68
0.473	130	19	1.002	0.198	1.029	26.2	42.2	9.96	8.03
3.993	136	20	1.002	0.198	1.013	1.67	35.3	5.94	2.68
0.473	190	21	1.002	0.198	1.007	1.13	36.9	5.59	1.16
0.506	170	19	1.002	0.198	0.992	9.86	40.3	7.83	3.75
0.604	190	22	1.002	0.198	1.013	0.494	34.0	4.90	1.00
0.477	176	24	1.002	0.198	1.018	5.02	37.5	6.35	2.31
2.459	130	24	1.002	0.198	0.993	19.7	36.5	9.03	5.30
4.008	138	27	1.002	0.198	0.999	1.18	36.2	5.96	2.54
7.767	190	18	0.420	0.099	3.208	0.174	19.7	2.00	0.426
4.005	130	19	0.128	1.002	0	13.4	34.1	8.00	4.41
0.628	190	18	0.094	0	6.404	12.4	39.8	4.67	7.15
3.396	190	18	0.229	0.798	0.101	0.404	28.4	2.62	1.73
5.824	130	21	1.085	0.662	6.679	7.86	35.8	8.26	4.74
8.730	130	20	2.798	0	9.780	0.522	31.9	4.66	0.740
8.730	130	20	3.001	0.846	10.010	0.424	32.2	2.89	0.601
6.800	130	24	3.001	0.846	10.012	0.304	34.5	3.32	0.711
19.994	180	20	2.482	1.002	9.999	0	0	0	0
20.018	180	20	2.475	0	0	0	0	0	0
20.018	180	20	2.482	1.002	0	0	0	0	0
20.018	180	20	2.475	0	9.996	0	0	0	0
22.054	190	19	0.505	1.002	10.008	0.028	0.348	0.025	0.003
22.054	190	19	0.505	1.002	0	0.483	4.26	0.332	0.067
22.054	190	19	0.498	0	9.999	0.893	8.85	0.685	0.086
22.054	190	19	0.498	0	0	0.211	6.84	0.461	0.011
21.180	130	17	0.511	0	9.990	9.79	34.1	9.26	5.39
3.736	144	19	2.999	0	0	14.2	33.0	7.17	3.26
5.147	152	17	1.950	0.005	2.627	1.19	34.0	5.10	0.931
23.985	144	16	2.999	0	0	0.756	22.1	2.16	0.472
1.307	170	20	0.501	0.099	2.001	3.32	42.0	6.77	3.57
1.307	170	20	2.007	0.099	0.507	0.975	32.5	3.41	0.403
3.557	170	20	0.511	0.402	2.001	0.687	34.0	5.29	2.56
24.011	130	19	0.504	0.997	9.357	1.93	35.8	7.52	4.31
12.517	162	21	2.376	0.260	10.004	0.162	14.4	0.868	0.074
16.128	158	20	2.618	0.260	8.560	0.559	12.8	0.700	0.143
0.979	130	19	2.775	0.926	10.005	19.2	36.8	9.02	5.86
0.979	130	19	2.562	1.002	9.998	18.7	37.4	9.48	6.13
0.979	130	19	3.001	0.846	9.994	19.3	37.0	8.92	5.95
16.128	158	20	2.609	0	0	0.166	10.8	0.489	0.097
16.128	158	20	2.618	0.260	0	0.163	10.5	0.428	0.099
16.128	158	20	2.609	0	8.562	0.217	13.1	0.840	0.164
12.517	162	21	2.381	0	0	0.203	12.3	0.606	0.062
12.517	162	21	2.376	0.260	0	0.184	14.6	0.794	0.086
12.517	162	21	2.381	0	9.995	0.274	16.9	0.900	0.080

^aCel = cellulose; GM = glucomannan

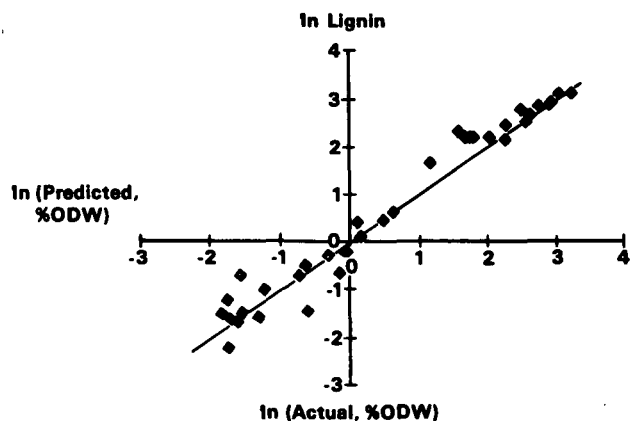


Fig. 3 Observed and predicted lignin yields.

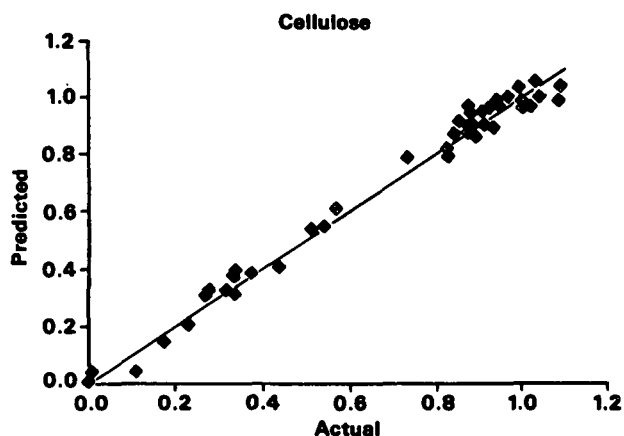


Fig. 4 Observed and predicted cellulose contents, normalized by wood cellulose content.

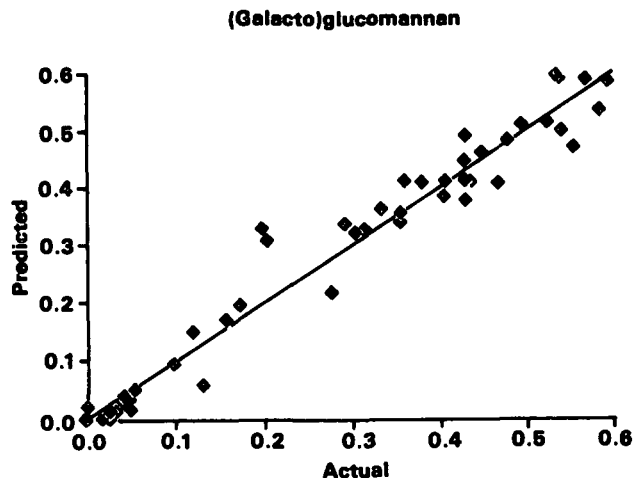


Fig. 5 Observed and predicted glucomannan contents, normalized by wood glucomannan content.

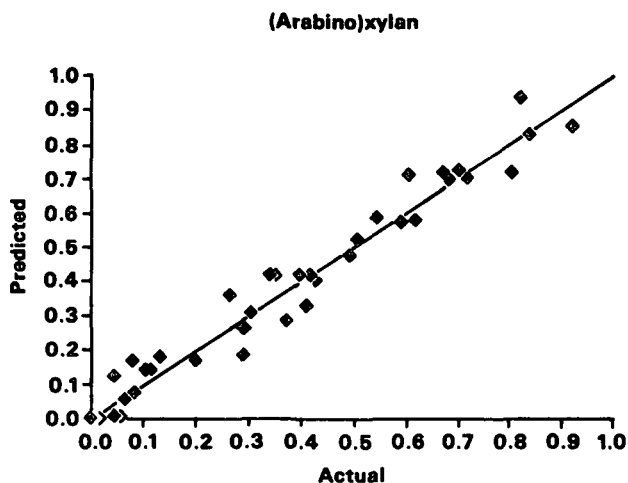


Fig. 6 Observed and predicted xylan contents, normalized by wood xylan content.